Journal of Medicinal Chemistry

Article

pubs.acs.org/jmc

Indazole-6-phenylcyclopropylcarboxylic Acids as Selective GPR120 Agonists with in Vivo Efficacy

William McCoull,*[,†] Andrew Bailey,[§] Peter Barton,[†] Alan M. Birch,[§] Alastair J. H. Brown,[§] Hayley S. Butler,[§] Scott Boyd,[†] Roger J. Butlin,[§] Ben Chappell,[§] Paul Clarkson,[†] Shelley Collins,[§] Robert M. D. Davies,[§] Anne Ertan,[§] Clare D. Hammond,[§] Jane L. Holmes,[§] Carol Lenaghan,[§] Anita Midha,[§] Pablo Morentin-Gutierrez,[†] Jane E. Moore,[§] Piotr Raubo,[†] and Graeme Robb[†]

[†]IMED Oncology and Discovery Sciences, AstraZeneca, 310 Cambridge Science Park, Milton Road, Cambridge, CB4 0WG, U.K.
[§]IMED CVMD, AstraZeneca, Mereside, Alderley Park, Macclesfield, SK10 4TG, U.K.

Supporting Information

ABSTRACT: GPR120 agonists have therapeutic potential for the treatment of diabetes, but few selective agonists have been reported. We identified an indazole-6-phenylcyclopropylcarboxylic acid series of GPR120 agonists and conducted SAR studies to optimize GPR120 potency. Furthermore, we identified a (*S*,*S*)-cyclopropylcarboxylic acid structural motif which gave selectivity against GPR40. Good oral exposure was obtained with some compounds displaying unexpected high CNS penetration. Increased MDCK efflux was utilized to identify compounds such as **33** with lower CNS penetration, and activity in oral glucose tolerance studies was demonstrated. Differential activity was observed in GPR120 null and wild-type mice indicating that this effect operates through a mechanism involving GPR120 agonism.

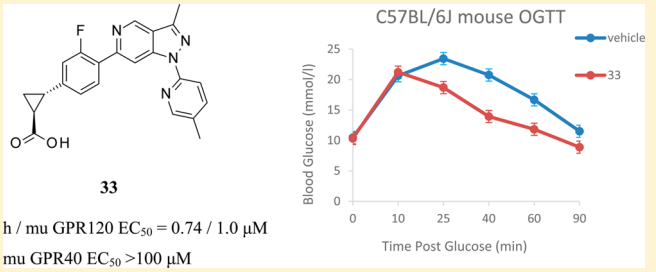

INTRODUCTION

Type 2 diabetes (T2D) is one of the fastest growing diseases worldwide and is estimated to affect 415 million in 2015.[1] One of the likely major reasons for this is unhealthy diet and lifestyle choices leading to obesity, insulin resistance, and elevated levels of free fatty acids in plasma.[2] The G-protein-coupled receptor GPR120, also known as the free fatty acid receptor 4 (FFAR4), has been suggested to act as a lipid sensor in the body, being implicated in a diversity of processes like adipogenesis, inflammation, and regulation of metabolic control. GPR120 is activated by medium and long chain fatty acids.[3] Dysfunction of GPR120 has been associated with development of obesity, and recently a mutation in the human GPR120 gene, inhibiting GPR120 signaling, was observed in obese subjects.[4] A GPR120 agonist has been shown to improve insulin resistance in obese mice,[5] and selective GPR120 agonists have therapeutic potential for the treatment of diabetes.[6,7] There are only a small number of GPR120 agonists reported, and obtaining high selectivity for GPR120 over a related lipid sensing GPCR, GPR40 (also known as FFAR1), has been challenging to achieve.[8−14] The GPR120 agonist TUG-891 (3-{4-[(4-fluoro-4′-methyl-2-biphenylyl)-methoxy]phenyl}propanoic acid) was shown to be selective over GPR40 in human forms of these receptors but exhibits limited selectivity against the murine form,[15] indicating that interspecies differences are also a challenge in the delivery of selective in vivo probes.

RESULTS AND DISCUSSION

A pyrazole **1** from the patent literature[16] known as "Metabolex 36"[17] was identified as an attractive starting point. We postulated that rigidification of the ether side chain by connecting from oxygen to the pyrazole through installation of an indazole ring as in **2** would present a novel GPR120 chemotype from which SAR exploration would be possible (Figure 1). A carboxylic acid is

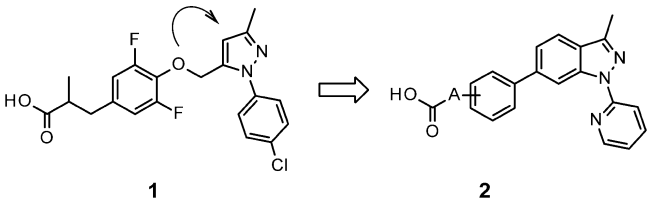

Figure 1. Scaffold hop strategy.

common in most known GPR120 agonists; thus we postulated that a carboxylic acid with an appropriate spacer group A from a phenyl group attached to the 6-position of the indazole as in **2** would result in desired GPR120 agonism. A 2-pyridyl substitutent was utilized rather than 4-chlorophenyl for the purposes of reducing overall lipophilicity.

Received: February 9, 2017

DOI: 10.1021/acs.jmedchem.7b00210
J. Med. Chem. XXXX, XXX, XXX−XXX

Table 1. Initial Indazole Lead and SAR Exploration

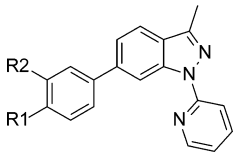

compd	R1	R2	h GPR120 Epic EC_{50} (μM)[a,b] (efficacy)	mu GPR40 FLIPR EC_{50} (μM)[a,c] (efficacy)
3	CH_2CO_2H	H	>17 (8)	
4	$CH_2CH_2CO_2H$	H	0.64 (107)	1.4 (95)
5	$CH_2CMe_2CO_2H$	H	4.1 (79)	>100 (18)
6	$CH_2CH_2CH_2CO_2H$	H	0.26 (128)	2.1 (117)
7	H	$CH_2CH_2CO_2H$	>17 (28)	>100 (0)
8	H	CH_2CO_2H	>17 (3)	

[a]Mean of at least two independent measurements. [b]pIC_{50} SEM is <0.14. [c]pIC_{50} SEM is <0.03.

Table 2. SAR Exploration of 6-Phenylindazole

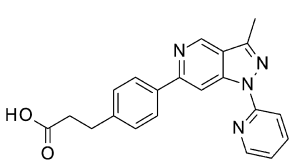

9

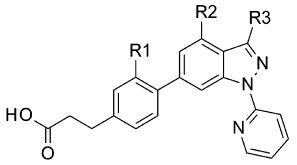

10-21

compd	R1	R2	R3	h GPR120 Epic EC_{50} (μM)[a,b] (efficacy)	mu GPR40 FLIPR EC_{50} (μM)[a,c] (efficacy)	log $D_{7.4}$
9				2.6 (78)	9.2 (86)	1.6
10	OMe	H	Me	0.72 (82)	8.2 (62)	2.4
11	CN	H	Me	2.4 (80)	6.1 (47)	2.2
12	F	H	Me	0.60 (113)	1.5 (105)	2.9
13	Cl	H	Me	0.71 (113)	1.2 (102)	3.3
14	H	H	H	0.99 (114)	4.5 (106)	2.4
15	H	H	OMe	0.25 (122)	2.6 (96)	3.3
16	H	H	OBn	>17 (2)	1.3 (81)	
17	H	H	Et	0.76 (75)	1.1 (93)	3.3
18	H	H	CN	4.8 (87)	2 (124)	3
19	H	Me	H	4.6 (70)	2.6 (82)[d]	2.6
20	H	F	H	0.47 (100)	2.6 (126)	2.8
21	H	CN	H	2.0 (78)	19 (113)	2.2

[a]Mean of at least two independent measurements unless otherwise stated. [b]pIC_{50} SEM is <0.31. [c]pIC_{50} SEM is <0.19. [d]n = 1.

GPR120 agonism was measured by looking at DMR (dynamic mass redistribution response) detected using Corning EPIC technology[18] for overexpressed human GPR120 in CHO cells. Since it was important to ultimately obtain selectivity against GPR40 not only in human but also in murine isoforms, then GPR40 agonism was measured by looking at intracellular calcium levels in FLIPR format for overexpressed mouse GPR40 in HEK293s cells. Although acetic acid analogue **3** was inactive, the propanoic acid **4** gave GPR120 agonism with EC_{50} = 0.64 μM, thus validating the indazole core as a GPR120 scaffold (Table 1). However, GPR40 agonism was also present for **4**. Further SAR was evident at the para-position, R1. Dimethyl substitution of the propanoic acid in **5** removed the GPR40 agonism with 6-fold reduction in GPR120 potency, suggesting that optimization for balance of GPR120 potency and selectivity could be achieved by substituted propanoic acid analogues. Butanoic acid **6** showed improved GPR120 potency but again with significant GPR40 activity. Propanoic acid (**7**) and ethanoic acid (**8**) analogues at the meta-position did not exhibit significant GPR120 agonism.

Having achieved both GPR120 and GPR40 agonism with propanoic acid **4**, we utilized this side chain to explore SAR for both receptors by modifying substitution on the indazole core (Table 2). Incorporation of nitrogen at the 5-position of the indazole gave **9** which modestly reduced GPR120 and GPR40 potency by 4- and 6-fold, respectively. Since this change was accompanied by a large reduction in log $D_{7.4}$ of 1.2, then it was considered of potential use in combination with other productive SAR elsewhere in the molecule later. A range of substituents was tolerated at the ortho-phenyl R1 position with relatively flat SAR (**10**−**13**). Methoxy, fluoro, and chloro gave similar GPR120 potency and selectivity compared to hydrogen. Cyano gave modestly reduced potency against both receptors. Removal of the methyl group at R3 was tolerated in **14**, and methoxy substitution modestly improved GPR120 potency 2.5-fold in **15** with increased selectivity against GPR40. Larger benzyloxy compound **16** was inactive against GPR120, although GPR40 agonism was maintained. Ethyl analogue **17** had similar GPR120 and GPR40 potency, as the methyl benchmark **4** and cyano analogue **18** reduced GPR120 potency 7.5-fold while maintaining GPR40 potency. Since R3 = H was well tolerated in **14**, substitution was varied at R2 while keeping R3 unsubstituted (**19**−**21**). Fluoro substitution at R2 emerged as giving the greatest GPR120 potency with cyano and methyl substitution being 5- and 10-fold lower.

DOI: 10.1021/acs.jmedchem.7b00210
J. Med. Chem. XXXX, XXX, XXX−XXX

Table 3. SAR Exploration of Ethyl Linker

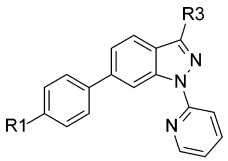

14, 22-23, 25-28

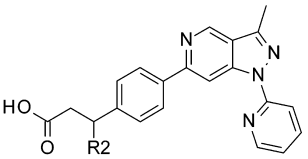

9, 24

Cpd	R1	R3	R2	h GPR120 Epic EC_{50} (μM)[a,b] (efficacy)	mu GPR40 FLIPR EC_{50} (μM)[a,c] (efficacy)
14	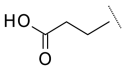	H		0.99 (114)	4.5 (106)
22	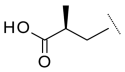 (*S*)	H		4 (100)	3.8 (31)
23	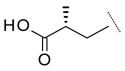 (*R*)	H		4.3 (88)	>100 (18)
9			H	2.6 (78)	9.2 (86)
24			Me	12 (28)	61 (50)
4	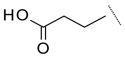	Me		0.64 (107)	1.4 (95)
25	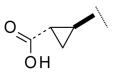 *trans*-racemic	Me		0.85 (87)	>100 (6)
26	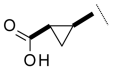 *cis*-racemic	Me		>17 (9)	19 (81)
27	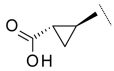 (*S*,*S*)	Me		0.69 (95)	>100 (10)
28	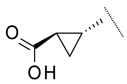 (*R*,*R*)	Me		>17 (26)	>100 (2)

[a]Mean of at least two independent measurements. [b]pIC_{50} SEM is <0.07 [c]pIC_{50} SEM is <0.15.

A parallel SAR exploration was conducted to explore substitution on the ethyl linker (Table 3). α-Methylation to the acid of **14** reduced GPR120 potency 4-fold and (*S*)-**22** maintained GPR40 potency while (*R*)-**23** was not active against GPR40, indicating that chirality at this position was important. β-Methylation to the acid of **9** reduced both GPR120 and GPR40 activity in **24**. This led us to postulate that the smallest possible α,β-disubstituted cyclopropyl analogues[19] were worth investigating. The *trans*-racemate **25** maintained GPR120 potency but was inactive against GPR40, while the *cis*-racemate **26** was inactive against GPR120 potency and weakly active against GPR40. Consequently, the enantiomers of *trans*-cyclopropyl were prepared and all GPR120 activity was found to reside with the (*S*,*S*)-**27** enantiomer while the (*R*,*R*)-**28** enantiomer was inactive.

DOI: 10.1021/acs.jmedchem.7b00210
J. Med. Chem. XXXX, XXX, XXX−XXX

Table 4. Selected Combination Compounds with (*S*,*S*) Cyclopropane Acid

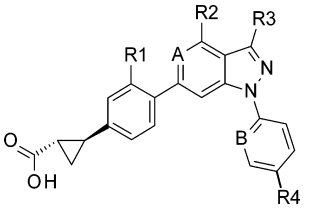

compd	A	R1	R2	R3	B	R4	h/mu GPR120 Epic EC_{50} (μM)[a,b] (efficacy)	mu GPR40 FLIPR EC_{50} (μM)[a] (efficacy)	log $D_{7.4}$
29	N	H	H	Me	CH	Me	0.90 (76)/0.64 (99)	>100 (12)	2.6
30	CH	H	F	Me	CH	Me	0.52 (88)/0.54 (112)	>100 (14)	4.2
31	CH	H	F	OMe	N	H	0.51 (93)/0.62 (103)	>100 (19)	3.8
32	CH	H	H	OMe	N	H	0.47 (102)/0.41 (99)	>100 (1)	3.8
33	N	F	H	Me	N	Me	0.74 (66)/1.0 (79)	>100 (2)	2.6
34	CH	H	H	Me	CH	Me	0.36 (100)/0.51 (91)	>100 (1)	3.8
35	CH	H	F	OMe	CH	Me	0.078 (115)/0.017[c] (176)	>100 (11)	>4.2

[a]Mean of at least two independent measurements unless otherwise stated. [b]pIC_{50} SEM is <0.22 [c]n = 1.

Scheme 1. General Synthesis of (*S*,*S*)-Indazole-6-phenylcyclopropylcarboxylic Acids[a]

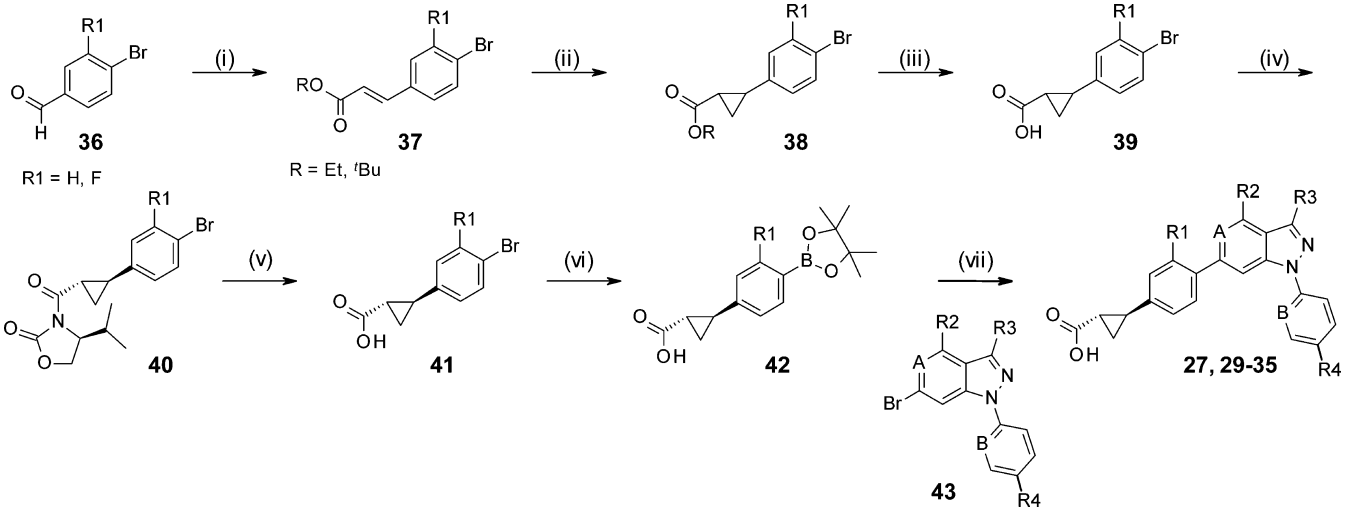

[a]Reagents and conditions: (i) $RO_2CCH_2P(O)(OEt)_2$, NaH, THF, R1 = H, 72%, R1 = F, 95%; (ii) $I(OSMe_3)$, ^{t}BuOK, DMSO, R1 = H, 70%, R1 = F, 61%. (iii) R1 = H, Et ester: LiOH, H_2O/THF, 93%. R1 = F, ^{t}Bu ester: TFA, DCM, 99%. (iv) Oxalyl chloride, NEt_3, (*S*)-4-isopropyloxazolidin-2-one, DCM, separate diastereomers, R1 = H, 27%, R1 = F, 34%; (v) LiOH, H_2O_2, H_2O/THF, R1 = H, 66%, R1 = F, 85%; (vi) 4,4,4′,4′,5,5,5′,5′-octamethyl-2,2′-bis(1,3,2-dioxaborolane), $Pd(dppf)Cl_2$, KOAc, 1,4-dioxane, R1 = H/F, 100%; (vii) Pd-118, K_3PO_4, H_2O/MeCN, 100 °C, microwave, 19−70%.

A specific cyclopropane configuration has also recently been identified as critical for GPR120 potency and selectivity over GPR40 within a different chemotype.[8]

The next SAR iteration involved combining some of the groups which improved potency of 6-phenylindazoles for GPR120 with the (*S*,*S*)-cyclopropanecarboxylic acid. The latter was expected to consistently give selectivity against GPR40, and this was achieved in all analogues (Table 4). For each of R1 and R2 either hydrogen or fluorine was selected, and for R3 either methyl or methoxy was selected. The pyridyl ring on the indazole nitrogen had not been altered throughout the SAR exploration, but other groups were expected to be tolerated; thus pyridyl, 4-methylpyridyl, and tolyl were selected to increase the diversity of structures. In addition, a nitrogen was introduced at the 5-position in **29** and **33** to further increase diversity of structure and also ADME properties by reduction of lipophilicity. Gratifyingly, the compounds all exhibited submicromolar potency against GPR120 and 4-fluoro-3-methoxyindazole **35** gave a significant increase in GPR120 potency at 78 nM. All compounds (**29**−**35**) were inactive in a null cell Epic assay and gave similar activity against the mouse isoform of GPR120, as the human isoform thus had potential to be in vivo probes (Table 4).

Synthesis. Synthesis of the (*S*,*S*)-indazole-6-phenylcyclopropylcarboxylic acid was conducted as shown in Scheme 1. Starting from the bromoaldehyde (**36**), the corresponding racemic 4-bromophenylcyclopropylcarboxylic acids (**39**) were obtained in the three-step sequence of reactions involving Horner−Wadsworth−Emmons olefination of **36** followed by Corey−Chaykovsky cyclopropanation of α,β-unsaturated ester **37** and hydrolysis of the ester **38** to corresponding racemic *trans*-cyclopropanecarboxylic acids **39**. Racemic **39** were converted to corresponding Evans' *N*-acyloxazolidinones, and diasteroisomers were separated by flash chromatography. The enantiomerically pure oxazolidinones **40** were subjected to hydrolysis and subsequently to palladium catalyzed boronylation with bis-(pinacolato)diboron to afford corresponding boronic esters **42**. In the next step, Suzuki−Miyaura cross-coupling reaction of **42** with corresponding heteroaryl halides **43** delivered homochiral

DOI: 10.1021/acs.jmedchem.7b00210
J. Med. Chem. XXXX, XXX, XXX−XXX

(*S*,*S*)-indazole-6-phenylcyclopropanecarboxylic acids (**27**, **29**–**35**).

In order to determine the absolute stereochemistry of the cyclopropyl group, a single crystal of **41** (R = H) was obtained and X-ray crystallographic analysis[20] showed (*S*,*S*) stereochemistry (Figure 2).

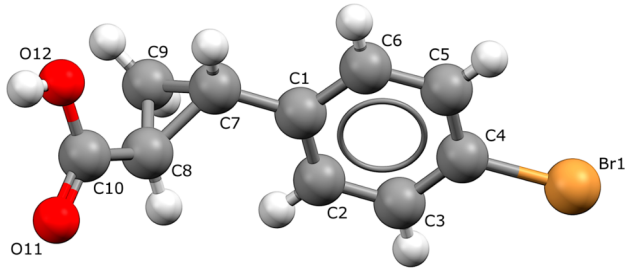

Figure 2. Perspective view of crystal structure of (*S*,*S*)-**41**.

The 6-haloindazole scaffolds were prepared as drawn in Scheme 2. *o*-Halobenzoic acids (**44**, **50**) were converted to corresponding ketone derivatives (**46**, **52**) via Wienreb amides **45** and **51**. Cyclization of **46** and **52** with hydrazine delivered expected haloindazole derivatives **47** and **53** in excellent yields. Copper catalyzed N-arylation of the indazole scaffolds with either boronic acids or 2-bromopyridines afforded 6-haloindazoles **48**, **49**, and **54**. The 3-methoxyindazole derivatives **60** were prepared starting from corresponding *o*-fluoromethylbenzoates **55**. Cycliszation of **55** with hydrazine followed by methylation of the hydroxy functionality using a Mitsunobu reaction and subsequent hydrolysis of the carbamate **58** provided the bromide **59**. Copper catalyzed N-arylation of **59** again provided bromides **60**.

Pharmacokinetic Properties and in Vivo Efficacy. For a number of compounds oral exposure in mouse was assessed and significant blood levels were obtained for most compounds (Table 5). On the basis of these data, sufficient free cover above the GPR120 potency was predicted at a dose of 100 mg/kg with **31**–**34** all having similar oral and intravenous properties. Although **35** had lower fraction unbound and lower bioavailability, higher potency led to greater free cover but concerns that lower solubility may result in nonlinearity of the oral exposure with increasing dose led us to prioritize **31**–**34** for further in vivo assessment. Dose escalation was conducted with **31** initially, and at 50 mg/kg maximum oral exposure of 97 μM was obtained which was in line with expected dose linearity. Increase of dose to

Scheme 2. General Synthesis of 6-Br-indazole Cores[a]

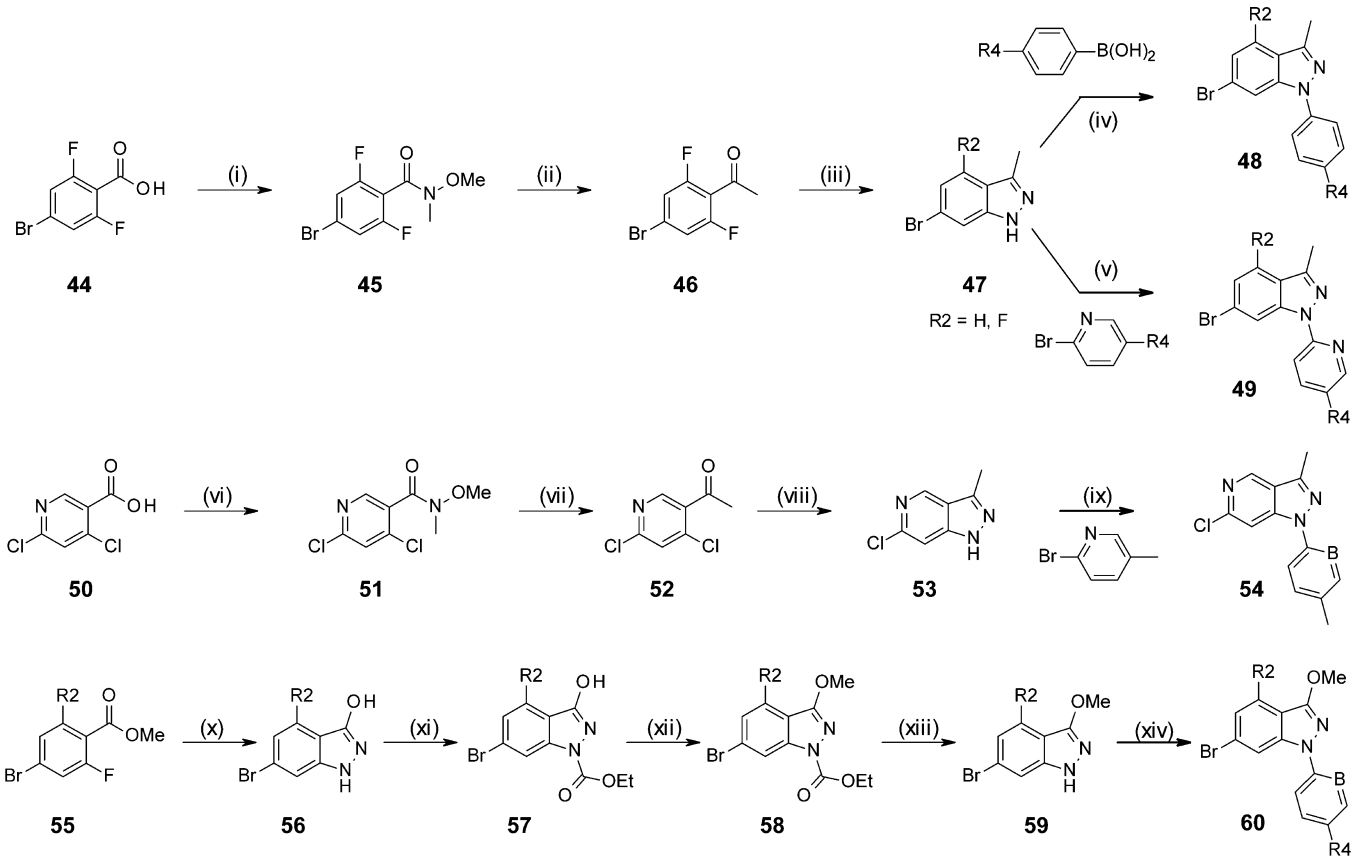

[a]Reagents and conditions: (i) oxalyl dichloride, DCM, then MeONHMe·HCl, NEt_3, 76%; (ii) MeMgBr, THF, 92%; (iii) $N_2H_4{\cdot}H_2O$, THF, 80 °C, 86%; (iv) $Cu(OAc)_2$, pyridine, DCM, R2 = H/R4 = Me 46%, R2 = F/R4 = Me 61%; (v) CuBr, K_2CO_3, *N*1,*N*2-dimethylethane-1,2-diamine, 1,4-dioxane, 105 °C, R2 = H/R4 = H, 50%; (vi) oxalyl dichloride, DCM, then MeONHMe·HCl, NEt_3, 79%; (vii) MeMgBr, THF, 99%; (viii) $N_2H_4{\cdot}H_2O$, Et_3N, ^{i}PrOH, 69%; (ix) CuBr, K_2CO_3, *N*1,*N*2-dimethylethane-1,2-diamine, 1,4-dioxane, 105 °C, B = N, 44%, B = CH, 81%; (x) $N_2H_4{\cdot}H_2O$, H_2O/THF, R2 = H, 98%, R2 = F, 100%; (xi) EtOCOCl, H_2O/pyridine, R2 = H, 73%, R2 = F, 86%; (xii) ^{i}PrO$_2$PN = NCO$_2{}^i$Pr, Ph_2Ppyridine or Ph_3P, MeOH, THF, R2 = H, 51%, R2 = F, 61%; (xiii) KOH, H_2O/EtOH, R2 = H, 90%, R2 = F, 91%; (xiv) conditions iv or v, 19–65%.

DOI: 10.1021/acs.jmedchem.7b00210
J. Med. Chem. XXXX, XXX, XXX−XXX

Table 5. Mouse Pharmacokinetic, Permeability and Efflux Data for Potential in Vivo Probes

compd	PPB % free	iv CL (mL min^{-1} kg^{-1})[a]	iv V_{ss} (L/kg)[a]	po C_{max} (μM)[b]	F (%)[a,b]	predicted free cover[c]	K_p[d]	$K_{p_{uu}}$[e]	Caco2 P_{app}(A–B) ($\times 10^{-6}$ cm/s)	MDCK-MDR1 efflux ratio[f]
31	0.53	5.2	1.0	8.2	159	1.4	2	0.45	29	0.59
32	0.48	9.3	1.5	5.4	126	1.3	2.3	0.86	31	2
33	2.1	13	2.4	3.3	131	1.4	0.37	0.14	76	2.8
34	0.49	9.6	1.2	7.9	136	1.5	0.82	0.22	58	5.1
35	0.11	0.4	0.7	5.0	19	6.4	0.44			

[a]Compound was dosed iv at 2.5 mg/kg (1 mg/kg for **33**) in 5% DMSO/95% hydroxypropyl β-cyclodextrin. [b]Compound was dosed po at 5 mg/kg in HPMC/Tween. [c]Calculated using po C_{max} at 5 mg/kg corrected for free fraction, scaled to 100 mg/kg and divided by GPR120 potency. [d]Ratio of the drug concentrations in homogenized brain tissue and blood, 2 h after po at 5 mg/kg in HPMC/Tween. [e]Calculated using free fraction measured in blood and brain (using rat brain slice method[22]). [f]Compound was incubated at 10 μM in cultured MDCK-MDR1 cells, and permeability was measured in both the A to B and B to A direction.

150 mg/kg was not tolerated by mice beyond 2 h. The animals became subdued and were terminated. Pharmacokinetic analysis from mice at the 2 h time point revealed that the blood exposure was 97 μM, the same as for the previously tolerated 50 mg/kg dose but CNS exposure was measured at 147 μM. It is not common for carboxylic acids to have such high CNS exposure as they are generally expected to have difficulty penetrating the blood–brain barrier;[21] hence this was an unexpected observation. At the same time dose escalation of **32** was conducted and it was tolerated at 150 mg/kg with blood exposure of 126 μM but at 300 mg/kg was not tolerated by mice beyond 1 h. In this case blood exposure was 284 μM and CNS exposure was 207 μM, again an unexpectedly high level in the brain for a carboxylic acid. We attributed the tolerability issue to be due to the large exposure levels in the brain and sought to profile compounds with lower CNS penetration.

We revisited low dose (5 mg/kg) oral exposure and confirmed that both **31** and **32** had significant CNS exposure at this dose with K_p values above 2 and, $K_{p_{uu}}$ values above 0.3. The $K_{p_{uu}}$ value is conceptually inversely related to the therapeutic index of peripheral drugs with potential CNS side effects;[22] thus we sought to decrease this parameter. All of our probe candidates had high intrinsic permeability measured using a Caco2 assay, but we have previously reported that modulation of efflux in an MDCK-MDR1 assay can be useful for predicting CNS exposure within a chemical series.[23] Consistent with their high CNS exposure **31** and **32** exhibited low efflux in this assay, but we were encouraged that **33** and **34** exhibited higher efflux and this translated into low CNS exposure with $K_{p_{uu}}$ values below 0.3. Consequently **33** and **34** were progressed to in vivo efficacy experiments

Both **33** and **34** were evaluated in an oral glucose tolerance test (OGTT) in C57BL/6J mice at 100 mg/kg and exhibited significant 45% ($p < 0.001$) and 65% ($p < 0.001$) reduction in blood glucose excursion following a 2 g/kg glucose load (Figure 3). The specificity of this efficacy was investigated using genetically altered mice lacking the GPR120 receptor (Figure 4). In the wild-type (WT) mice, similar reductions (47% ($p < 0.001$) for **33**, 58% ($p < 0.001$) for **34**) on blood glucose excursion occurred. However, in the null (KO) mice, no significant effects on blood glucose excursion were observed, confirming that the efficacy of **33** and **34** is mediated by GPR120. The link between efficacy and pharmacokinetics for OGTT is well understood,[24] and pharmacokinetic data from this study revealed that the exposure levels in WT and KO mice for each compound were similar and free blood exposure similar to the GPR120 EC_{50} was achieved (Figure 5). Lower brain exposure (as predicted from the earlier low dose pharmacokinetic studies) was

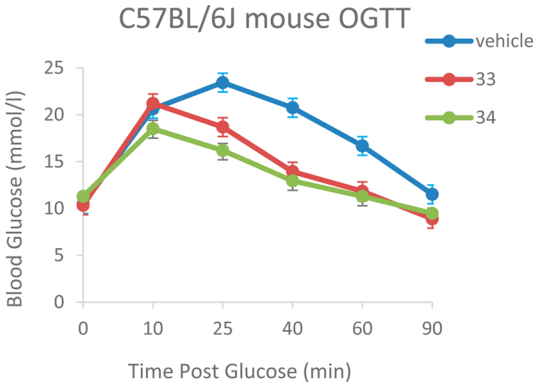

Figure 3. Glucose lowering efficacy of **33** and **34** in mice.

obtained with **33** exhibiting $K_{p_{uu}} = 0.12$ and **34** exhibiting $K_{p_{uu}} = 0.27$.

Furthermore, in vitro pharmacological profiling[25] of **32** and **33** against a panel of over 30 diverse targets was conducted and exhibited excellent selectivity profiles (see Supporting Information). No targets showed activity below 1 μM, and one target for each compound showed activity below 10 μM (**32**, phosphodiesterase 4D $IC_{50} = 1.6$ μM; **33**, adenosine receptor A2α, $K_i = 1.7$ μM). Thus, we have not identified an off-target activity that could explain the tolerability issue of **32** at 300 mg/kg. Taking all these data together, **33** and **34** are excellent in vivo tool compounds for exploring the agonist pharmacology of the GPR120. They have been utilized to show that GPR120 is selectively present within the δ cells of murine islets and regulate somatostatin secretion,[26] and further studies will be reported in due course. Furthermore, a recent publication has highlighted the role of GPR120 agonism in the brain with food intake and reward behavior in mice,[27] and compounds such as **31** and **32** could be utilized at a tolerated dose to further explore the CNS effects of selective GPR120 agonists.

CONCLUSION

Starting from a scaffold hop, a new GPR120 agonist indazole chemotype was identified. SAR exploration was conducted and a (*S*,*S*)-cyclopropylcarboxylic acid structural motif identified which gave selectivity against GPR40. Further SAR optimization led to identification of several selective GPR120 agonists with good oral exposure. Unexpected high CNS exposure was encountered for some compounds, and increased MDCK-MDR1 efflux was used to identify compounds with reduced CNS exposure. Two tool compounds, **33** ((1*S*,2*S*)-2-(3-fluoro-4-(3-methyl-1-(5-methylpyridin-2-yl)-1*H*-pyrazolo[4,3-*c*]pyridin-6-

DOI: 10.1021/acs.jmedchem.7b00210
J. Med. Chem. XXXX, XXX, XXX–XXX

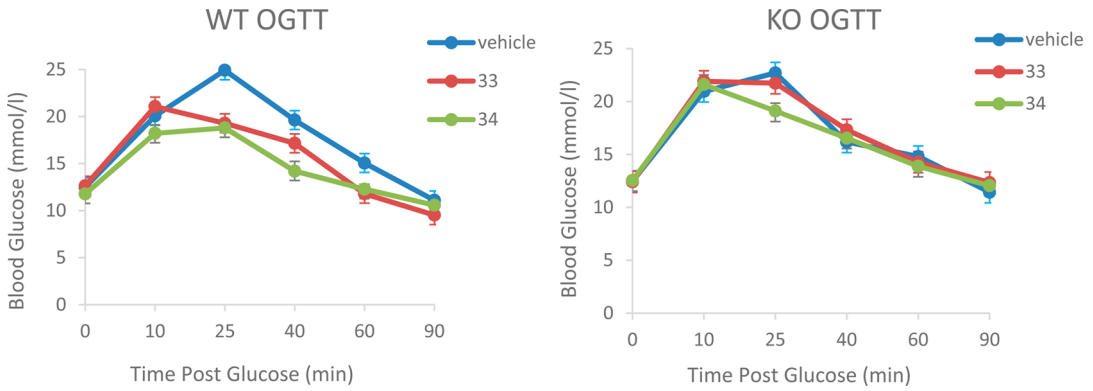

Figure 4. Glucose lowering efficacy of **33** and **34** in WT/KO GPR120 mice at 100 mg/kg.

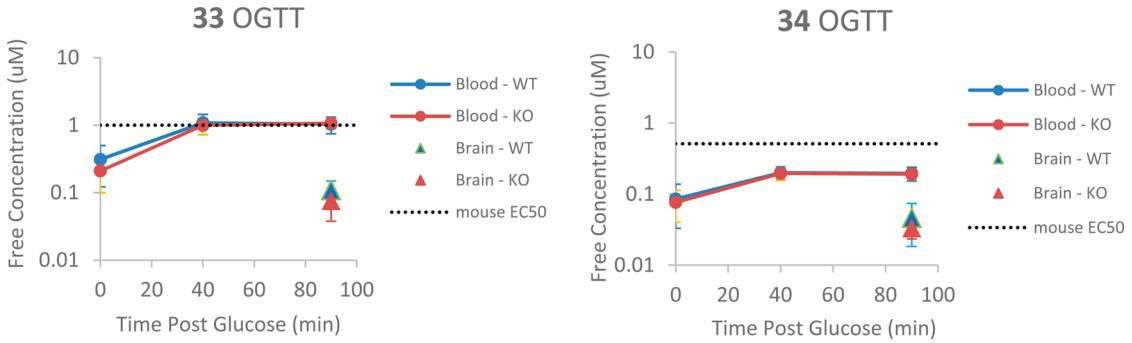

Figure 5. Blood and brain exposure of **33** and **34** in WT/KO GP R120 mice.

yl)phenyl)cyclopropanecarboxylic acid, AZ13595491) and **34** ((1*S*,2*S*)-2-(4-(3-methyl-1-*p*-tolyl-1*H*-indazol-6-yl)phenyl)-cyclopropanecarboxylic acid, AZ13595423) were progressed to in vivo studies and demonstrated significant reduction in blood glucose excursion in response to a glucose challenge. This efficacy was reproduced in GPR120 WT mice but not in KO mice, indicating that this effect occurs through a mechanism involving GPR120 agonism.

EXPERIMENTAL SECTION

General. All solvents and chemicals used were reagent grade. Anhydrous solvents THF, benzene, DCE, DCM, and DME were purchased from Aldrich. Flash column chromatography was carried out using prepacked silica cartridges (from 4 g up to 330 g) from Redisep or Silicycle and eluted using an Isco Companion system. Purity and characterization of compounds were established by a combination of liquid chromatography−mass spectrometry (LC−MS), gas chromatography−mass spectrometry (GC−MS), and NMR analytical techniques, and purity was >95% for all test compounds. ^{1}H NMR results were recorded on a Varian INOVA (600 MHz), Varian Gemini 2000 (300 MHz), or Bruker Avance DPX400 (400 MHz) and were determined in $CDCl_3$ or DMSO-d_6. Chemical shifts are reported in ppm relative to TMS (0.00 ppm) or solvent peaks as the internal reference. Splitting patterns are indicated as follows: s, singlet; d, doublet; t, triplet; m, multiplet; br, broad peak. Elevated temperatures were used where necessary to sharpen broad NMR peaks due to rotamers, and the temperature used is noted for such compounds. Merck precoated TLC plates (silica gel 60 F_{254}, 0.25 mm, art. 5715) were used for TLC analysis. Solutions were dried over anhydrous magnesium sulfate, and the solvent was removed by rotary evaporation under reduced pressure.

Synthesis of Representative Key Examples (33 and 34). (*E*)-*tert*-Butyl 3-(4-Bromo-3-fluorophenyl)acrylate (37, R1 = F, ^{t}Bu Ester). Sodium hydride (0.90 g, 22.5 mmol) was added portionwise to 4-bromo-3-fluorobenzaldehyde (4.15 g, 20.4 mmol) and *tert*-butyl 2-(diethoxyphosphoryl)acetate (6.19 g, 24.5 mmol) in THF (100 mL) at rt over a period of 10 min under nitrogen. The resulting yellow mixture was stirred at rt for 1.5 h. The reaction mixture was quenched with saturated NH_4Cl (50 mL), water (50 mL) and diluted with EtOAc (150 mL), and the organic layer was separated, dried over $MgSO_4$, filtered, and evaporated. The crude product was purified by flash silica chromatography, with elution gradient 0−5% EtOAc in heptane. Pure fractions were evaporated to dryness to afford the title compound (5.82 g, 95%) as a white solid. ^{1}H NMR (400 MHz, $CDCl_3$) δ 1.53 (9H, s), 6.36 (1H, d), 7.15 (1H, dd), 7.23−7.27 (1H, m), 7.47 (1H, d), 7.55 (1H, dd).

***trans*-(1*S*,2*S*)/(1*R*,2*R*)-*tert*-Butyl 2-(4-Bromo-3-fluorophenyl)-cyclopropanecarboxylate (38, R1 = F, ^{t}Bu Ester).** Trimethylsulfoxonium iodide (0.950 g, 4.32 mmol) was added in one portion to potassium *tert*-butoxide (0.461 g, 3.98 mmol) in DMSO (10 mL) at rt under nitrogen. The resulting suspension was heated to 50 °C and stirred for 1.5 h. The solution was cooled to rt, and a solution of **37** (R1 = F, ^{t}Bu ester) (1 g, 3.32 mmol) in DMSO (5 mL) was added dropwise over 1 h. The reaction was stirred at rt for 5 h and then neutralized with saturated NH_4Cl and extracted with 25% EtOAc in heptane. The organic layer was dried over $MgSO_4$, filtered, and evaporated to afford crude product which was purified by flash silica chromatography, with elution gradient 0−4% EtOAc in heptane. Pure fractions were evaporated to dryness to afford the title compound (0.64 g, 61%) as a colorless oil. ^{1}H NMR (400 MHz, $CDCl_3$) 1.18 (1H, ddd), 1.47 (9H, s), 1.53−1.58 (1H, m), 1.80 (1H, ddd), 2.36−2.42 (1H, m), 6.77 (1H, dd), 6.83 (1H, dd), 7.42 (1H, dd).

***trans*-(1*S*,2*S*)/(1*R*,2*R*)-2-(4-Bromo-3-fluorophenyl)-cyclopropanecarboxylic Acid (39, R1 = F).** **38** (R1 = F, ^{t}Bu ester) (6.67 g, 21.2 mmol) was solvated by DCM (70 mL). To this solution was added TFA (30 mL). The resulting solution was stirred at rt for 1 h, and then solvent was removed under reduced pressure. The residue was then azeotroped with toluene to provide the title compound (5.45 g, 99%) as a white solid. ^{1}H NMR (400 MHz, DMSO-d_6) δ 1.32−1.5 (2H, m), 1.87 (1H, ddd), 2.44 (1H, ddd), 7.02 (1H, dd), 7.22 (1H, dd), 7.52−7.63 (1H, m), 12.34 (1H, s); *m*/*z* $(M - H)^-$ = 259.

(*S*)-3-((1*S*,2*S*)-2-(4-Bromo-3-fluorophenyl)cyclopropane-carbonyl)-4-isopropyloxazolidin-2-one (40, R1 = F). Oxalyl dichloride (1.90 mL, 22.1 mmol) was added dropwise to **39** (R1 = F)

DOI: 10.1021/acs.jmedchem.7b00210
J. Med. Chem. XXXX, XXX, XXX−XXX

(5.45 g, 21.0 mmol) and DMF (8.15 μL, 0.11 mmol) in DCM (43 mL) under nitrogen. The resulting mixture was stirred at rt for 2 h. The reaction mixture was evaporated to dryness and azeotroped with toluene. The resulting crude acid chloride was dissolved in DCM (43 mL). Triethylamine (5.87 mL, 42.1 mmol) was added followed by portionwise addition of (*S*)-4-isopropyloxazolidin-2-one (2.72 g, 21.0 mmol). The mixture was stirred at rt under nitrogen for 18 h. The reaction mixture was diluted with DCM and washed sequentially with water and saturated brine. The organic layer was filtered through a phase separation cartridge and evaporated. The crude product was purified by flash silica chromatography, with elution gradient 40% heptane in DCM. Pure fractions were evaporated to dryness to afford the title compound as white solid (2.66 g, 34%). ^{1}H NMR (400 MHz, DMSO-d_6) δ 0.80 (3H, d), 0.85 (3H, d), 1.49−1.69 (2H, m), 2.17 (1H, ddq), 2.51−2.6 (1H, m), 3.40 (1H, ddd), 3.99−4.56 (3H, m), 7.02 (1H, dd), 7.26 (1H, dd), 7.5−7.84 (1H, m); m/z $(M + H)^+$ = 372.

(1*S*,2*S*)-2-(4-Bromo-3-fluorophenyl)cyclopropanecarboxylic Acid (41, R1 = F). Hydrogen peroxide (50 wt %, 2.36 mL, 28.7 mmol) was added dropwise to a solution of lithium hydroxide hydrate (0.482 g, 11.5 mmol) in water (5 mL) at rt. The resulting solution was stirred for 30 min and then cooled to 0 °C. This cooled solution was added portionwise to a cooled solution of **40** (R1 = F) (2.66 g, 7.18 mmol) in THF (24 mL) and water (5 mL). The internal temperature remained below 10 °C throughout the addition. The resulting solution was stirred for 2 h. Sodium sulfite (3.62 g, 28.7 mmol) in water (24 mL) was added. The mixture was extracted with EtOAc (2 × 50 mL). The aqueous phase was acidified with 2 M HCl, extracted with EtOAc (3 × 60 mL) and the combined organic layers were dried over $MgSO_4$, filtered, and evaporated to afford a colorless oil. This was purified by ion exchange chromatography, using a PE AX column (20 g). The product was eluted from the column using 5% formic acid/MeCN. Solvent was then removed under reduced pressure to provide the title compound (1.58 g, 85%). ^{1}H NMR (400 MHz, DMSO-d_6) δ 1.28−1.55 (2H, m), 1.87 (1H, ddd), 2.36−2.46 (1H, m), 7.01 (1H, dd), 7.22 (1H, dd), 7.48−7.64 (1H, m), 12.34 (1H, s); m/z $(M - H)^-$ = 257

(1*S*,2*S*)-2-(4-(4,4,5,5-Tetramethyl-1,3,2-dioxaborolan-2-yl)-3-fluorophenyl)cyclopropanecarboxylic Acid (42, R1 = F). Potassium acetate (957 mg, 9.75 mmol), **41** (R1 = F) (842 mg, 3.25 mmol), 4,4,4′,4′,5,5,5′,5′-octamethyl-2,2′-bi(1,3,2-dioxaborolane) (908 mg, 3.58 mmol), and 1,1′-bis(diphenylphosphino)ferrocenepalladium-(II) dichloride DCM complex (131 mg, 0.16 mmol) were suspended in degassed 1,4-dioxane (12 mL). The resulting suspension was evacuated and purged with nitrogen 5 times and then heated to 90 °C for 16 h. The reaction mixture was filtered through Celite, washing through with DCM, then THF. The filtrate was concentrated to provide the title compound (995 mg, 100%), which was used without further purification. m/z $(M - H)^-$ = 305.

4,6-Dichloro-*N*-methoxy-*N*-methylnicotinamide (51). Oxalyl dichloride (4.60 mL, 52.6 mmol) was added portionwise to a suspension of 4,6-dichloronicotinic acid (10.1 g, 52.6 mmol) in DCM (150 mL)/DMF (3 mL) at 0 °C over a period of 3 min under nitrogen. The resulting suspension was stirred at 0 °C for 10 min and then allowed to warm to rt and stirred for a further 16 h. The solvent was evaporated in vacuo to yield 4,6-dichloronicotinoyl chloride which was used directly in the next reaction without further purification. ^{1}H NMR (400 MHz, $CDCl_3$) δ 7.53 (1H, s), 9.09 (1H, s). 4,6-Dichloronicotinoyl chloride (1.15 g, 5.47 mmol) in DCM (10 mL) was added to an ice-bath-cooled mixture of *N*,*O*-dimethylhydroxylamine hydrochloride (0.8 g, 8.21 mmol), triethylamine (2.67 mL, 19.2 mmol), and DCM (15 mL). The cooling batch was removed, and the mixture was stirred at rt for 7 h and left overnight on standing. The reaction mixture was quenched with saturated aqueous $NaHCO_3$ (25 mL), extracted with DCM (2 × 25 mL), and the organic layer was dried and evaporated. The crude product was purified by flash silica chromatography, with elution gradient 10−50% EtOAc in heptane. Pure fractions were evaporated to dryness to afford the title compound (1.01g, 79%) as a gum. ^{1}H NMR (400 MHz, $CDCl_3$) δ 3.40 (3H, s), 3.50 (3H, s), 7.45 (1H, s), 8.37 (1H, s); m/z $(M + H)^+$ = 237.

1-(4,6-Dichloropyridin-3-yl)ethanone (52). Methylmagnesium bromide (1.4 M in toluene/THF (3:1), 67.7 mL, 94.8 mmol) was added portionwise to a stirred solution of **51** (10.1 g, 43.1 mmol) in THF (100 mL) at 0 °C under nitrogen. The resulting suspension was stirred at 0 °C for 2 h. The reaction mixture was quenched with saturated aqueous NH_4Cl (50 mL) and then extracted with EtOAc (100 mL). The organic layer was washed with brine (50 mL) and then dried ($MgSO_4$), filtered, and evaporated to yield the title compound (8.09 g, 99%). ^{1}H NMR (400 MHz, DMSO-d_6) δ 2.64 (3H, s), 7.93 (1H, s), 8.80 (1H, s); m/z $(M + H)^+$ = 190.

6-Chloro-3-methyl-1*H*-pyrazolo[4,3-*c*]pyridine (53). Hydrazine hydrate (1.86 mL, 24.4 mmol) was added to a mixture of **52** (4.04 g, 21.3 mmol) and triethylamine (2.96 mL, 21.3 mmol) and isopropanol (13.8 mL) at rt under nitrogen. The resulting mixture was stirred at reflux for 16 h. The reaction mixture was then diluted with EtOAc/*n*-butanol (1:1) and washed with sat. aq $NaHCO_3$. The aqueous phase was separated, and the organics were dried over $MgSO_4$, filtered, and concentrated to small volume. The precipitate was filtered, washed with small amount of DCM, and dried under vacuum to afford the title compound (2.45 g, 69%) as a pale yellow solid. ^{1}H NMR (400 MHz, DMSO-d_6) δ 2.54 (3H, s), 7.51 (1H, d), 8.87 (1H, d), 13.25 (1H, s); m/z $(M + H)^+$ = 168.

6-Chloro-3-methyl-1-(5-methylpyridin-2-yl)-1*H*-pyrazolo-[4,3-*c*]pyridine (54, B = N). Potassium carbonate (1.11 g, 8.06 mmol) was added to **53** (1 g, 5.97 mmol), 2-bromo-5-methylpyridine (1.54 g, 8.95 mmol), *N*1,*N*2-dimethylethylene-1,2-diamine (1.05 mL, 8.35 mmol), and copper(I) bromide (0.428 g, 2.98 mmol) in 1,4-dioxane (20 mL). The resulting mixture was stirred at 105 °C for 2 h under nitrogen. The reaction was cooled to rt. EtOAc was added and the mixture filtered through Celite and evaporated to dryness to afford a crude product. The crude product was triturated with hot EtOH to give a solid which was collected by filtration and dried under vacuum to give the title compound (0.68 g, 44%) as a white solid. ^{1}H NMR (400 MHz, DMSO-d_6) δ 2.34 (3H, s), 2.64 (3H, s), 7.77−7.85 (2H, m), 8.35−8.4 (1H, m), 8.47 (1H, d), 8.99 (1H, d); m/z $(M + H)^+$ = 259.

(1*S*,2*S*)-2-(3-Fluoro-4-(3-methyl-1-(5-methylpyridin-2-yl)-1*H*-pyrazolo[4,3-*c*]pyridin-6-yl)phenyl)cyclopropanecarboxylic Acid (33). A mixture of **54** (B = N) (184 mg, 0.71 mmol), **42** (R1 = F) (218 mg, 0.71 mmol), tetrakis(triphenylphosphine)palladium(0) (82 mg, 0.07 mmol), isopropanol (3 mL), and sat. aq sodium bicarbonate (0.75 mL) was degassed and heated within a microwave reactor at 120 °C for 4 h. The reaction mixture was then passed through a PL-thiol MP SPE 500 mg/6 mL cartridge, eluting with EtOH, then MeOH/DCM. The filtrate was concentrated under reduced pressure. The crude product was purified by preparative HPLC (Waters XBridge Prep C18 OBD column, 5 μm silica, 50 mm diameter, 150 mm length), using decreasingly polar mixtures of water (containing 0.5% ammonia) and MeCN as eluents. Fractions containing the desired compound were evaporated to dryness to afford the title compound (109 mg, 38%). ^{1}H NMR (400 MHz, DMSO-d_6) δ 1.23 (1H, t), 1.35−1.43 (1H, m), 1.79−1.88 (1H, m), 2.33 (4H, m), 2.68 (3H, s), 7−7.19 (2H, m), 7.74−7.89 (2H, m), 7.94 (1H, t), 8.38 (1H, s), 8.89 (1H, s), 9.22 (1H, d); ^{13}C NMR (126 MHz, DMSO-d_6) 12.2, 17.5, 17.7, 25.1, 25.4, 109.1 (d, J = 10.9 Hz) 112.7, 114.0 (d, J = 24.5 Hz), 121.5, 122.7 (d, J = 2.7 Hz), 125.4 (d, J = 10.9 Hz) 130.4, 131.6 (d, J = 2.7 Hz), 140.0, 142.6, 144.7 (d, J = 8.2 Hz), 144.9, 145.7, 148.2, 149.0 (d, J = 2.7 Hz), 151.4, 160.3 (d, J = 248.0 Hz), 174.3; m/z $(M + H)^+$ = 403. HRMS (ES^+) for $C_{23}H_{20}FN_4O_2$ (MH^+): calcd 403.1570; found, 403.1556. $\alpha_D^{24.7}$ +187.9 (*c* 0.62, EtOH).

(*E*)-Ethyl 3-(4-Bromophenyl)acrylate (37, R1 = H, Et Ester). Ethyl 2-(diethoxyphosphoryl)acetate (24.2 g, 108 mmol) was added dropwise to a suspension of sodium hydride (6.49 g, 162 mmol) in THF (125 mL) at 0 °C over a period of 20 min. The resulting solution was allowed to warm to rt and stirred for 1 h, cooled to 0 °C and a solution of 4-bromobenzaldehyde (10 g, 54.0 mmol) in THF (50 mL) added dropwise over a period of 15 min. The resulting solution was stirred at rt for 30 h. The reaction mixture was poured into saturated brine (750 mL), extracted with EtOAc (3 × 250 mL). The combined organic phases were dried over Na_2SO_4, filtered, and evaporated to afford a yellow liquid. This was purified by flash silica chromatography, with elution gradient 0−5% EtOAc in petroleum ether. Pure fractions were evaporated to dryness to afford the title compound (10 g, 72%) as a pale yellow liquid. ^{1}H NMR (300 MHz, DMSO-d_6) δ 1.25 (3 H, t), 4.18 (2

DOI: 10.1021/acs.jmedchem.7b00210
J. Med. Chem. XXXX, XXX, XXX−XXX

H, q), 6.65 (1 H, d), 7.49−7.75 (5 H, m). HRMS (TOF) for $C_{13}H_{15}O_2Br$ (M^+): calcd, 282.0255; found, 282.0272.

***trans*-(1*S*,2*S*)/(1*R*,2*R*)-Ethyl 2-(4-Bromophenyl)cyclopropanecarboxylate (38, R1 = H, Et Ester).** Trimethylsulfoxonium iodide (56.1 g, 255 mmol) was added in one portion to potassium *tert*-butoxide (27.8 g, 235 mmol) in DMSO (405 mL) at rt under nitrogen. The resulting suspension was heated to 50 °C and stirred for 1 h. The pale yellow solution was cooled to rt, and a solution of **37** (R1 = H, Et ester) (50 g, 196 mmol) in DMSO (135 mL) was added dropwise over 1 h. The reaction was stirred at rt overnight. The reaction mixture was diluted with diethyl ether and washed with saturated aqueous NH_4Cl. The organic layer was dried over $MgSO_4$, filtered, and evaporated to afford the title compound (36.8 g, 70%) as a yellow oil which was used without further purification. ^{1}H NMR (400 MHz, DMSO-d_6) δ 1.19 (3H, t), 1.36 (1H, ddd), 1.41−1.5 (1H, m), 1.93 (1H, ddd), 2.42 (1H, ddd), 4.05−4.13 (2H, m), 7.11−7.17 (2H, m), 7.41−7.47 (2H, m).

***trans*-(1*S*,2*S*)/(1*R*,2*R*)-2-(4-Bromophenyl)cyclopropanecarboxylic Acid (39, R1 = H).** Lithium hydroxide hydrate (9.99 g, 238 mmol) was added to **38** (R1 = H, Et ester) (21.4 g, 79.4 mmol) in THF (225 mL) and water (75 mL). The resulting mixture was stirred at rt overnight. The reaction mixture was diluted with water (125 mL) and washed with diethyl ether (125 mL). The organic phase was extracted with water (60 mL). The combined aqueous phases were acidified with 2 M HCl (aq). The resulting suspension was extracted with DCM (600 mL). The organic phase was filtered through a phase separation cartridge and evaporated to afford the title compound (17.8 g, 93%) as a cream solid. ^{1}H NMR (400 MHz, DMSO-d_6) δ 1.32 (1H, ddd), 1.42 (1H, ddd), 1.77−1.84 (1H, m), 2.38 (1H, ddd), 7.13 (2H, d), 7.44 (2H, d), 12.30 (1H, s); m/z $(M - H)^-$ = 241.

(*S*)-3-((1*S*,2*S*)-2-(4-Bromophenyl)cyclopropanecarbonyl)-4-isopropyloxazolidin-2-one (40, R1 = H). Oxalyl dichloride (6.67 mL, 77.7 mmol) was added dropwise to **39** (R1 = H) (17.8 g, 74.0 mmol) and DMF (0.03 mL, 0.37 mmol) in DCM (150 mL) under nitrogen. The resulting mixture was stirred at rt for 1.5 h. The reaction mixture was evaporated to dryness and azeotroped with toluene. The resulting crude acid chloride was dissolved in DCM (150 mL). Triethylamine (20.6 mL, 148 mmol) was added followed by portionwise addition of (*S*)-4-isopropyloxazolidin-2-one (9.56 g, 74.0 mmol). The mixture was stirred at rt under nitrogen for 64 h. The reaction mixture was diluted with DCM and washed sequentially with water and saturated brine. The organic layer was filtered through a phase separation cartridge and evaporated. The crude product was purified by flash silica chromatography,with elution gradient 20% heptane in DCM. Pure fractions were evaporated to dryness to afford the title compound as a white solid after trituration with ether/heptane (7.13 g, 27%). ^{1}H NMR (400 MHz, DMSO-d_6) δ 0.79 (3H, d), 0.84 (3H, d), 1.49 (1H, ddd), 1.59 (1H, ddd), 2.16 (1H, dp), 3.38 (1H, ddd), 4.25−4.35 (2H, m), 4.39 (1H, dt), 7.12−7.18 (2H, m), 7.43−7.48 (2H, m).

(1*S*,2*S*)-2-(4-Bromophenyl)cyclopropanecarboxylic Acid (41, R1 = H). Hydrogen peroxide (50 wt %, 2.03 mL, 35.2 mmol) was added dropwise to a solution of lithium hydroxide hydrate (0.591 g, 14.1 mmol) in water (8 mL) at rt. The resulting solution was stirred for 30 min and then cooled to 0 °C. This cooled solution was added portionwise to a cooled solution of **40** (R1 = H) (3.1 g, 8.80 mmol) in THF (40 mL) and water (10 mL). The internal temperature remained below 10 °C throughout the addition. The resulting solution was stirred for 3.5 h. Sodium sulfite (4.44 g, 35.2 mmol) in water (20 mL) was added. The mixture was extracted with EtOAc (2 × 50 mL). The aqueous phase was then acidified with 2 M HCl. The aqueous phase was extracted with EtOAc (3 × 60 mL) and the combined organic layers were dried over $MgSO_4$, filtered, and evaporated to afford crude product. This was recrystallized from diethyl ether/heptane to give the title compound (1.39 g, 66%). ^{1}H NMR (400 MHz, DMSO-d_6) δ 1.31 (1H, ddd), 1.42 (1H, ddd), 1.80 (1H, ddd), 2.38 (1H, ddd), 7.1−7.15 (2H, m), 7.41−7.46 (2H, m), 12.29 (1H, s); m/z $(M - H)^-$ = 241.

(1*S*,2*S*)-2-(4-(4,4,5,5-Tetramethyl-1,3,2-dioxaborolan-2-yl)-phenyl)cyclopropanecarboxylic Acid (42, R1 = H). Potassium acetate (330 mg, 3.36 mmol), **41**, R1 = H (270 mg, 1.12 mmol), 4,4,4′,4′,5,5,5′,5′-octamethyl-2,2′-bi(1,3,2-dioxaborolane) (313 mg, 1.23 mmol), and 1,1′-bis(diphenylphosphino)ferrocenepalladium(II) dichloride DCM complex (45.7 mg, 0.06 mmol) were suspended in degassed 1,4-dioxane (3 mL). The resulting suspension was evacuated and purged with nitrogen 5 times and then heated to 90 °C for 5 h. The reaction mixture was filtered through Celite, washing through with DCM, then THF. The filtrate was concentrated to provide the title compound (625 mg, 100%), which was used without further purification. ^{1}H NMR (400 MHz, DMSO-d_6) δ 1.15 (6H, s), 1.22−1.31 (6H, m), 1.61−1.71 (1H, m), 1.72−1.78 (1H, m), 2.11−2.22 (1H, m), 3.59 (1H, t), 7.06 (2H, d), 7.52 (1H, d); m/z $(M - H)^-$ = 287.

6-Bromo-3-methyl-1-*p*-tolyl-1*H*-indazole (48, R2 = H, R4 = Me). Copper(II) acetate (2.58 g, 14.2 mmol) was added to a stirred mixture of 6-bromo-3-methyl-1*H*-indazole (2.00 g, 9.48 mmol), *p*-tolylboronic acid (1.93 g, 14.2 mmol), pyridine (2.3 mL, 28.4 mmol), and DCM (40 mL). The mixture was stirred at rt for 4 h under air. 35% ammonia solution (25 mL) was added, and the mixture was stirred for 15 min. The organic layer was separated and concentrated in vacuo. The crude product was purified by flash silica chromatography, with elution gradient 0−5% EtOAc in heptane. Pure fractions were evaporated to dryness and solid was washed with a small amount of diethyl ether to afford the title compound (1.32 g, 46%) as a solid. ^{1}H NMR (400 MHz, DMSO-d_6) δ 2.38 (3H, s), 2.57 (3H, s), 7.33−7.4 (3H, m), 7.57−7.62 (2H, m), 7.80 (1H, d), 7.89 (1H, d); m/z $(M + H)^+$ = 301.

(1*S*,2*S*)-2-(4-(3-Methyl-1-*p*-tolyl-1*H*-indazol-6-yl)phenyl)-cyclopropanecarboxylic Acid (34). 1,1′-Bis(di-*tert*-butylphosphino)ferrocenepalladium(II) dichloride (19 mg, 0.03 mmol) and tripotassium phosphate (251 mg, 1.2 mmol) were added to **42** (R1 = H) (138 mg, 0.48 mmol) and **48** (R2 = H, R4 = Me) (120 mg, 0.40 mmol) in degassed MeCN (1 mL) and water (1 mL) at 20 °C under nitrogen. The resulting mixture was further degassed and stirred within a microwave reactor at 100 °C for 1 h. The reaction mixture was acidified with acetic acid (0.25 mL) and extracted into DCM/MeOH (9:1 mixture). The organic phase was passed through a PL-thiol MP SPE 500 mg/6 mL cartridge, and the solid was washed with a 9:1 mixture of DCM/MeOH. The filtrate was concentrated. The crude product was purified by preparative HPLC (Waters XBridge Prep C18 OBD column, 5 μm silica, 50 mm diameter, 150 mm length), using decreasingly polar mixtures of water (containing 0.5% ammonia) and MeCN as eluents. Fractions containing the desired compound were evaporated to dryness to afford the title compound (106 mg, 70%) as solid. ^{1}H NMR (400 MHz, DMSO-d_6) δ 1.38 (1H, ddd), 1.46 (1H, dt), 1.82−1.88 (1H, m), 2.38 (3H, s), 2.41−2.46 (1H, m), 2.59 (3H, s), 7.27 (2H, d), 7.37 (2H, d), 7.49 (1H, dd), 7.66 (4H, dd), 7.83 (1H, s), 7.88 (1H, d), 12.28 (1H, s); ^{13}C NMR (126 MHz, DMSO-d_6) 12.1, 17.2, 21.0, 24.8, 25.5, 108.1, 120.9, 121.6, 122.3, 124.0, 127.0, 127.8, 130.5, 135.8, 137.8, 138.8, 139.8, 139.9, 140.3, 143.6, 174.3; m/z $(M + H)^+$ = 383. HRMS (ES^+) for $C_{25}H_{23}N_2O_2$ (MH^+): calcd 383.1760; found, 383.1742. $\alpha_D^{24.5}$ +204.8 (*c* 0.62, EtOH).

Biological Protocols. Human and Mouse GPR120 Dynamic Mass Redistribution (DMR) Assays. CHO FlpIn cryopreserved cells stably expressing human or mouse GPR120 were seeded in 30 μL of growth medium (DMEM/F-12 glutaMAX, 10% FCS, and 300 μg/mL hygromycin) into 384-well Corning EPIC fibronectin coated plates 48 h prior to assay and incubated at 37 °C in a CO_2 incubator. The growth medium was changed, 24 h prior to assay, to 30 μL of medium containing no serum, and the plates were returned to the CO_2 incubator. The medium was again changed, 2 h prior to assay, to 30 μL of assay buffer containing 0.5% DMSO (HBSS, 20 mM HEPES, 0.01% BSA at pH 7.4), and the plates were returned to the CO_2 incubator. Plates were equilibrated in the EPIC instrument and multiple baseline measurements were taken over a period of 10 min prior to adding 15 μL of test or control substance to the wells. Following addition, further measurements were taken over a period of 15 min to establish the agonist effect of test substance on the DMR of the cells.

Test compounds were administered to the plates in duplicate in a 10-point concentration−response format with final concentrations from 16 μM to 0.8 nM. Two control agonist compounds were assessed in each assay run to determine interassay variability. Each plate contained 32 maximum and minimum controls. A maximal concentration of a control agonist compound was used to define the assay maximum. The minimum control wells received 15 μL of assay buffer and DMSO

DOI: 10.1021/acs.jmedchem.7b00210
J. Med. Chem. XXXX, XXX, XXX−XXX

instead of test compound. Test compound effects were analyzed and represented in concentration−response format as percentage effect versus maximum control.

Active compounds were also tested for nonspecific activity using a CHO FlpIn null cell line in the same assay technology using the same protocol.

Mouse GPR40 Calcium Mobilization Assay. HEK293s cryopreserved cells stably expressing mouse GPR40 were seeded in 40 μL of growth medium (DMEM glutaMAX, 10% FCS, and 800 μg/mL G418) into 384 well poly-D-lysine plates 24 h prior to assay and incubated at 37 °C in a CO_2 incubator. The growth medium was carefully replaced, 1 h prior to assay, with 30 μL per well of calcium 3 loading solution, and the plates were returned to the CO_2 incubator. For each plate the loading solution was prepared by adding 100 μL of calcium 3 stock (see molecular devices calcium 3 stock formulation) and 6 μL of 2 mM FLUO-4 AM to 12 mL of assay buffer (HBSS, 20 mM HEPES, 0.01% BSA, probenecid 2.5 mM at pH 7.4). Plates were equilibrated in the fluometric imaging plate reader (FLIPR) Tetra instrument, and 10 baseline measurements were taken prior to adding 15 μL of test or control substance to the wells. Following addition, further measurements were taken over a period of 5 min to establish the agonist effect of test substance on calcium mobilization in the cells.

Test compounds were administered to the plates in duplicate in a 9-point concentration−response format with final concentrations from 100 μM to 7 nM. Two control agonist compounds were assessed in each assay run to determine interassay variability. Each plate contained 32 maximum and minimum controls. A maximal concentration of a control agonist compound (eladic acid) was used to define the assay maximum. The minimum control wells received 15 μL of assay buffer and DMSO instead of test compound. Test compound effects were analyzed and represented in concentration− response format as percentage effect versus maximum control.

Compounds were also tested for antagonist activity in the same assay by subsequently introducing an EC_{80} concentration of eladic acid to the wells and analyzing for inhibition of the agonist effect.

Mouse OGTT. Standard and combination OGTT studies were carried out using in-house C57BL/6J mice aged 10−11 weeks. GPR120 receptor KO and WT control mice were also bred in house, back-crossed onto a C57BL/6J background, and used at 9−10 weeks of age. For each experiment a concentrated stock of compound suspension was formulated at rt the day before study and diluted on day of study to the required dose concentrations. Powder was wetted and dispersed in vehicle by stirring and vortexing. Particle size reduction to <10 μm diameter was achieved by sonication for 15−20 min in an ultrasonic water bath and stirring overnight on a magnetic stirrer. Overnight (18 h) fasted mice were dosed via oral gavage (10 mL/kg) with either vehicle (HPMC/Tween) or compound. At 30 min after compound a 2 g/kg oral glucose load (10 mL/kg of 20% glucose in water) was administered. Tail prick blood samples were taken precompound (time −30), preglucose (time 0), and at 10, 25, 40, 60, and 90 min after glucose load to assess the glucose excursion profile. Glucose levels were measured on a Roche AccuChek hand-held monitor. Individual mouse glucose response AUCs (variable baseline), normalized to preglucose challenge (0 min) values, were calculated. The study was conducted on two separate occasions in order to assess reproducibility of the data, and data sets from both experiments were combined to enhance statistical power. Compound treated AUCs were compared to vehicle control by ANCOVA analysis. One sided Student *t* test for a decreasing effect using pooled interanimal variability was used. Time 0 blood glucose was used as covariate to account for differences in individual baseline glucose before glucose loading. Study day was included as a covariate to take into account any day effects. Differences with *p*-values of <0.05 were considered to be significant.

Pharmacokinetics. Pharmacokinetic studies were performed in male C57BL/6J and CD-1 mice. Intravenous (iv) administration was via bolus administration in a vehicle containing 5% DMSO 95% hydroxypropyl-β-cyclodextrin 30% (w/v). Oral dosing was administered by gavage in a vehicle containing HPMC/Tween. Blood samples were collected over a 24 h period postdose into tubes containing EDTA-K2. Noncompartmental analysis was performed to estimate pharmacokinetic parameters using WinNonLin (version 5.0.1). For brain/blood drug concentrations, animals were euthanized at 2 h postdose, and terminal blood and brain samples were collected from each animal and analyzed as previously described.[28] All animal experiments were conducted with strict adherence to licenses issued under the U.K. Animals (Scientific Procedures) Act 1986 and after local ethical review and approval.

■ ASSOCIATED CONTENT

Supporting Information

The Supporting Information is available free of charge on the ACS Publications website at DOI: 10.1021/acs.jmedchem.7b00210.

Preparation and additional characterization for final compounds; effect of **33** and **32** in in vitro radioligand binding, enzyme and funtional assays (PDF)

Molecular formula strings (CSV)

■ AUTHOR INFORMATION

Corresponding Author

*Phone: +44(0)1625236807. E-mail: william.mccoull@astrazeneca.com.

ORCID

William McCoull: 0000-0002-2977-1744

Notes

The authors declare no competing financial interest.

■ ACKNOWLEDGMENTS

Alex Brough, Alex Brien, Mike Harding, Ewan Coates, Rebecca Ruscoe, Mike Harding, and Trystan Nicholls are thanked for synthesis contributions. Jenny Morrell and Steve Bloor are thanked for expert technical assistance in generating biological assay data. Scott Edmondson, Dave Smith, and Ruth MacDonald are thanked for useful discussions on this manuscript.

■ ABBREVIATIONS USED

EtOAc, ethyl acetate; FFAR1, free fatty acid receptor 1; FFAR4, free fatty acid receptor 4; GPR40, G-protein-coupled receptor 40; GPR120, G-protein-coupled receptor 120; MDCK, Madin−Darby canine kidney; MeCN, acetonitrile; OGTT, oral glucose tolerance test

■ REFERENCES

(1) Information about T2D can be found in the 2015 7th edition of the IDF Diabetes Atlas at the Web site of the International Diabetes Federation. http://www.diabetesatlas.org (accessed February 6, 2017).

(2) Boden, G. Obesity and free fatty acids. *Endocrinol. Metab. Clin. North Am.* **2008**, *37*, 635−646.

(3) Hirasawa, A.; Tsumaya, K.; Awaji, T.; Katsuma, S.; Adachi, T.; Yamada, M.; Sugimoto, Y.; Miyazaki, S.; Tsujimoto, G. Free fatty acids regulate gut incretin glucagon-like peptide-1 secretion through GPR120. *Nat. Med.* **2005**, *11*, 90−94.

(4) Ichimura, A.; Hirasawa, A.; Poulain-Godefroy, O.; Bonnefond, A.; Hara, T.; Yengo, L.; Kimura, I.; Leloire, A.; Liu, N.; Iida, K.; Choquet, H.; Besnard, P.; Lecoeur, C.; Vivequin, S.; Ayukawa, K.; Takeuchi, M.; Ozawa, K.; Tauber, M.; Maffeis, C.; Morandi, A.; Buzzetti, R.; Elliott, P.; Pouta, A.; Jarvelin, M. R.; Korner, A.; Kiess, W.; Pigeyre, M.; Caiazzo, R.; Van Hul, W.; Van Gaal, L.; Horber, F.; Balkau, B.; Levy-Marchal, C.; Rouskas, K.; Kouvatsi, A.; Hebebrand, J.; Hinney, A.; Scherag, A.; Pattou, F.; Meyre, D.; Koshimizu, T.; Wolowczuk, I.; Tsujimoto, G.; Froguel, P. Dysfunction of lipid sensor GPR120 leads to obesity in both mouse and human. *Nature* **2012**, *483*, 350−354.

(5) Oh, D. Y.; Walenta, E.; Akiyama, T. E.; Lagakos, W. S.; Lackey, D.; Pessentheiner, A. R.; Sasik, R.; Hah, N.; Chi, T. J.; Cox, J. M.; Powels, M.

DOI: 10.1021/acs.jmedchem.7b00210
J. Med. Chem. XXXX, XXX, XXX−XXX

A.; Di Salvo, J.; Sinz, C.; Watkins, S. M.; Armando, A. M.; Chung, H.; Evans, R. M.; Quehenberger, O.; McNelis, J.; Bogner-Strauss, J. G.; Olefsky, J. M. A Gpr120-selective agonist improves insulin resistance and chronic inflammation in obese mice. *Nat. Med.* **2014**, *20*, 942−947.

(6) Cornall, L. M.; Mathai, M. L.; Hryciw, D. H.; McAinch, A. J. GPR120 agonism as a countermeasure against metabolic diseases. *Drug Discovery Today* **2014**, *19*, 670−679.

(7) Yu, Y. Y.; Chen, C.; Kong, F. F.; Zhang, W. Clinicopathological significance and potential drug target of RUNX3 in breast cancer. *Drug Des., Dev. Ther.* **2014**, *8*, 2423−2430.

(8) Adams, G. L.; Velazquez, F.; Jayne, C.; Shah, U.; Miao, S.; Ashley, E. R.; Madeira, M.; Akiyama, T. E.; Di Salvo, J.; Suzuki, T.; Wang, N.; Truong, Q.; Gilbert, E.; Zhou, D.; Verras, A.; Kirkland, M.; Pachanski, M.; Powles, M.; Yin, W.; Ujjainwalla, F.; Venkatraman, S.; Edmondson, S. D. Discovery of chromane propionic acid analogues as selective agonists of GPR120 with in vivo activity in rodents. *ACS Med. Chem. Lett.* **2017**, *8*, 96−101.

(9) Azevedo, C. M.; Watterson, K. R.; Wargent, E. T.; Hansen, S. V.; Hudson, B. D.; Kepczynska, M. A.; Dunlop, J.; Shimpukade, B.; Christiansen, E.; Milligan, G.; Stocker, C. J.; Ulven, T. Non-acidic free fatty acid receptor 4 agonists with antidiabetic activity. *J. Med. Chem.* **2016**, *59*, 8868−8878.

(10) Cox, J. M.; Chu, H. D.; Chelliah, M. V.; Debenham, J. S.; Eagen, K.; Lan, P.; Lombardo, M.; London, C.; Plotkin, M. A.; Shah, U.; Sun, Z.; Vaccaro, H. M.; Venkatraman, S.; Suzuki, T.; Wang, N.; Ashley, E. R.; Crespo, A.; Madeira, M.; Leung, D. H.; Alleyne, C.; Ogawa, A. M.; Souza, S.; Thomas-Fowlkes, B.; Di Salvo, J.; Weinglass, A.; Kirkland, M.; Pachanski, M.; Powles, M. A.; Tozzo, E.; Akiyama, T. E.; Ujjainwalla, F.; Tata, J. R.; Sinz, C. J. Design, synthesis, and evaluation of novel and selective G-protein coupled receptor 120 (GPR120) spirocyclic agonists. *ACS Med. Chem. Lett.* **2017**, *8*, 49−54.

(11) Hara, T.; Hirasawa, A.; Sun, Q.; Sadakane, K.; Itsubo, C.; Iga, T.; Adachi, T.; Koshimizu, T. A.; Hashimoto, T.; Asakawa, Y.; Tsujimoto, G. Novel selective ligands for free fatty acid receptors GPR120 and GPR40. *Naunyn-Schmiedeberg's Arch. Pharmacol.* **2009**, *380*, 247−255.

(12) Lombardo, M.; Bender, K.; London, C.; Plotkin, M. A.; Kirkland, M.; Mane, J.; Pachanski, M.; Geissler, W.; Cummings, J.; Habulihaz, B.; Akiyama, T. E.; Di Salvo, J.; Madeira, M.; Pols, J.; Powles, M. A.; Finley, M. F.; Johnson, E.; Roussel, T.; Uebele, V. N.; Crespo, A.; Leung, D.; Alleyne, C.; Trusca, D.; Lei, Y.; Howard, A. D.; Ujjainwalla, F.; Tata, J. R.; Sinz, C. J. Discovery of benzofuran propanoic acid GPR120 agonists: From uHTS hit to mechanism-based pharmacodynamic effects. *Bioorg. Med. Chem. Lett.* **2016**, *26*, 5724−5728.

(13) Shimpukade, B.; Hudson, B. D.; Hovgaard, C. K.; Milligan, G.; Ulven, T. Discovery of a potent and selective GPR120 agonist. *J. Med. Chem.* **2012**, *55*, 4511−4515.

(14) Suzuki, T.; Igari, S.; Hirasawa, A.; Hata, M.; Ishiguro, M.; Fujieda, H.; Itoh, Y.; Hirano, T.; Nakagawa, H.; Ogura, M.; Makishima, M.; Tsujimoto, G.; Miyata, N. Identification of G protein-coupled receptor 120-selective agonists derived from PPARgamma agonists. *J. Med. Chem.* **2008**, *51*, 7640−7644.

(15) Hudson, B. D.; Shimpukade, B.; Mackenzie, A. E.; Butcher, A. J.; Pediani, J. D.; Christiansen, E.; Heathcote, H.; Tobin, A. B.; Ulven, T.; Milligan, G. The pharmacology of TUG-891, a potent and selective agonist of the free fatty acid receptor 4 (FFA4/GPR120), demonstrates both potential opportunity and possible challenges to therapeutic agonism. *Mol. Pharmacol.* **2013**, *84*, 710−725.

(16) Ma, J.; Novack, A.; Nashashibi, I.; Pham, P.; Rabbat, C. J.; Song, J.; Shi, D. F.; Zhao, Z.; Choi, Y.-J.; Chen, X. [(Heterocyclylmethoxy)-aryl]alkanoic acid derivatives as GPR120 receptor agonists and preparation and uses thereof. Patent WO2010/048207, 2010.

(17) Holliday, N. D.; Watson, S.-J.; Brown, A. J. H. Drug discovery opportunities and challenges at G protein coupled receptors for long chain free Fatty acids. *Front. Endocrinol.* **2012**, *2*, 112.

(18) Lee, P. H.; Gao, A.; van Staden, C.; Ly, J.; Salon, J.; Xu, A.; Fang, Y.; Verkleeren, R. Evaluation of dynamic mass redistribution technology for pharmacological studies of recombinant and endogenously expressed g protein-coupled receptors. *Assay Drug Dev. Technol.* **2008**, *6*, 83−94.

(19) Talele, T. T. The "cyclopropyl fragment" is a versatile player that frequently appears in preclinical/clinical drug molecules. *J. Med. Chem.* **2016**, *59*, 8712−8756.

(20) Molecular formula = $C_{10}H_9BrO_2$. Formula weight = 241.08. Crystal system = orthorhombic. Space group = $P2_12_12_1$, a = 6.5493(4) Å, b = 6.9515(5) Å, c = 20.6297(14) Å, α = 90°, β = 90°, γ = 90°, V = 939.218 Å^3, T = 200K, Z = 4, D_c = 1.705 gcm^{-1}, $\lambda_{(Mo\text{-}K\alpha)}$ = 0.71073, μ = 4.338 mm^{-1}, 3188 reflections measured, 2243 independent reflections, 1754 observed reflections [$I > 2.0\sigma(I)$], $R[F^2 > 2\sigma(F^2)]$ = 0.0293, goodness of fit = 1.027. Flack's x parameter = 0.014(14), indicating correctly defined chirality. Crystallographic data have been deposited with the Cambridge Crystallographic Data Centre as supplementary publication number CCDC 1530875.

(21) Pajouhesh, H.; Lenz, G. R. Medicinal chemical properties of successful central nervous system drugs. *NeuroRx* **2005**, *2*, 541−553.

(22) Friden, M.; Ducrozet, F.; Middleton, B.; Antonsson, M.; Bredberg, U.; Hammarlund-Udenaes, M. Development of a high-throughput brain slice method for studying drug distribution in the central nervous system. *Drug Metab. Dispos.* **2009**, *37*, 1226−1233.

(23) McCoull, W.; Barton, P.; Brown, A. J.; Bowker, S. S.; Cameron, J.; Clarke, D. S.; Davies, R. D.; Dossetter, A. G.; Ertan, A.; Fenwick, M.; Green, C.; Holmes, J. L.; Martin, N.; Masters, D.; Moore, J. E.; Newcombe, N. J.; Newton, C.; Pointon, H.; Robb, G. R.; Sheldon, C.; Stokes, S.; Morgan, D. Identification, optimization, and pharmacology of acylurea GHS-R1a inverse agonists. *J. Med. Chem.* **2014**, *57*, 6128−6140.

(24) Gabrielsson, J.; Hjorth, S.; Vogg, B.; Harlfinger, S.; Gutierrez, P. M.; Peletier, L.; Pehrson, R.; Davidsson, P. Modeling and design of challenge tests: inflammatory and metabolic biomarker study examples. *Eur. J. Pharm. Sci.* **2015**, *67*, 144−159.

(25) Bowes, J.; Brown, A. J.; Hamon, J.; Jarolimek, W.; Sridhar, A.; Waldron, G.; Whitebread, S. Reducing safety-related drug attrition: the use of in vitro pharmacological profiling. *Nat. Rev. Drug Discovery* **2012**, *11*, 909−922.

(26) Stone, V. M.; Dhayal, S.; Brocklehurst, K. J.; Lenaghan, C.; Sorhede Winzell, M.; Hammar, M.; Xu, X.; Smith, D. M.; Morgan, N. G. GPR120 (FFAR4) is preferentially expressed in pancreatic delta cells and regulates somatostatin secretion from murine islets of Langerhans. *Diabetologia* **2014**, *57*, 1182−1191.

(27) Auguste, S.; Fisette, A.; Fernandes, M. F.; Hryhorczuk, C.; Poitout, V.; Alquier, T.; Fulton, S. Central agonism of GPR120 acutely inhibits food intake and food reward and chronically suppresses anxiety-like behavior in mice. *Int. J. Neuropsychopharmacol.* **2016**, *19*, pyw014.

(28) Goldberg, F. W.; Dossetter, A. G.; Scott, J. S.; Robb, G. R.; Boyd, S.; Groombridge, S. D.; Kemmitt, P. D.; Sjogren, T.; Gutierrez, P. M.; deSchoolmeester, J.; Swales, J. G.; Turnbull, A. V.; Wild, M. J. Optimization of brain penetrant 11beta-hydroxysteroid dehydrogenase type I inhibitors and in vivo testing in diet-induced obese mice. *J. Med. Chem.* **2014**, *57*, 970−986.

DOI: 10.1021/acs.jmedchem.7b00210
J. Med. Chem. XXXX, XXX, XXX−XXX